Sensibility analysis of the FO CRS traveltime approximation

Pedro Chira-Oliva(*), João C. R. Cruz(*) Steffen Bergler(†) and Peter Hubral(†)

(*) Federal University of Pará (Brazil), chira, jcarlos@ufpa.br

(†) Geophysical Institute of Karlsruhe (Germany), steffen.bergler, peter.hubral@gpi.uni-karlsruhe.de

This paper was prepared for presentation at the 8th International Congress of The Brazilian Geophysical Society held in Rio de Janeiro, Brazil, 14-18 September 2003.

Abstract

The 2-D finite-offset (FO) Common-Reflection-Surface (CRS) stack simulates a specified 2-D finite-offset (FO) section (e.g., a common-offset (CO) section), and is able to handle P-P, S-S reflections and P-S or S-P converted reflections, respectively. Also large-offset reflections can be utilized in this process. This approach depends on five stacking parameters: two angles and three wavefront curvatures, which are determined from the seismic data by means of a coherence analysis. These parameters are related to kinematic wavefield attributes useful in several problems. The five kinematic wavefield attributes can be considered for further use in inversion, e.g., macro-model inversion and Amplitude-versus-Offset (AVO) analysis. In this paper we investigate the sensibility of the FO CRS stacking operator with respect to the kinematic data-derived attributes. By analysing the first derivative of the FO CRS traveltime with respect to each one of the searched-for parameters, we describe the behavior of the FO CRS stacking surface.

Introduction

In recent years, stacking methods as the POLYSTACK (e.g. de Bazelaire (1988)), Multifocusing (e.g. Gelchinsky et al. (1999a,b); Landa et al. (1999)) and the Common-Reflection-Surface (CRS) (e.g. Mann et al. (1999); Jäger et al. (2001); Trappe et al. (2001)) have gained a new importance in seismic process. These techniques have been used to stack P-P reflection events in 2-D pre-stack multi-coverage data and to simulate zero-offset sections. To handle also converted reflections in the frame of the CRS stack, the zero-offset (ZO) CRS stack has been generalized to stack pre-stack data into a selected FO section (Zhang et al., 2001).

The FO CRS stacking operator is constituted by five parameters, which have to be searched-for in a coherence-based, data-driven way (Zhang et al., 2001). The FO CRS stack has demonstrated the applicability not only to P-P or S-S reflections, but also to seismic multi-coverage data containing converted reflections, where the emergence angle information provided by the FO CRS stack can be used to reliably separate P-P from P-S reflections. The inline geometrical spreading factor can, for instance, be computed from the attributes, which is of help for AVO analysis (Bergler et al., 2001a). The FO CRS stack parameters may be used to determine in a subsequent traveltime inversion the P-wave velocity and/or S-wave velocity of a layered earth model (Bergler et al., 2001b).

As part of the inverse problem, we describe the behavior of the FO CRS stack surface, by analysing the first derivative of the FO traveltime approximation with respect to each of the searched-for parameters.

Basic Theory

The FO CRS stacking operator (Zhang et al., 2001) for converted and non-converted reflections in dependence of midpoint (x_m) and half-offset (h) coordinates of the paraxial ray (Figure 1) is given by

$$\begin{aligned} t^2 = & \left[t_0 + \left(\frac{\sin\beta_G}{v_G} + \frac{\sin\beta_S}{v_S})(x_m - x_0)\right)\right. \\ & \left. + \left(\frac{\sin\beta_G}{v_G} - \frac{\sin\beta_S}{v_S}\right)(h-h_0)\right]^2 \\ & + 2t_0\left[\left(K_3\frac{\cos^2\beta_G}{v_G} + K_2\frac{\cos^2\beta_S}{v_S}\right)(h-h_0)\right. \\ & + \frac{1}{2}\left(K_3\frac{\cos^2\beta_G}{v_G} - K_2\frac{\cos^2\beta_S}{v_S}\right)(h-h_0)^2 \\ & \left. + \left((4K_1 - 3K_3)\frac{\cos^2\beta_G}{v_G} - K_2\frac{\cos^2\beta_S}{v_S}\right)\frac{(x_m-x_0)^2}{2}\right], \end{aligned} \quad (1)$$

where t_0 is the reflection traveltime along the central ray. x_0 and h_0 being the midpoint and half-offset coordinates of the central ray. x_m and h are the midpoint and half-offset coordinates of the paraxial ray. β_S and β_G are the incidence angle and the emergence angle of the central ray at the source S and the receiver G, respectively (Figure 1). v_S and v_G are the wave velocities at the source and receiver, respectively. K_1 is the resulting wavefront curvature at the receiver G in the seismic line of a wave emanated from a point source S and traveled along the central ray in the real common-shot (CS) experiment (Figure 2). K_2 and K_3 are the wavefront curvatures of a fictitious wave at source S and receiver G of the central ray, respectively, where each paraxial ray that starts at the coordinate $x_0 - h$ on the seismic line emerges after reflection at the coordinate $x_0 + h$ in the hypothetical common-midpoint (CMP) experiment (see Figure 2). Formula (1) represents a second-order traveltime approximation of paraxial rays in the vicinity of the central ray.

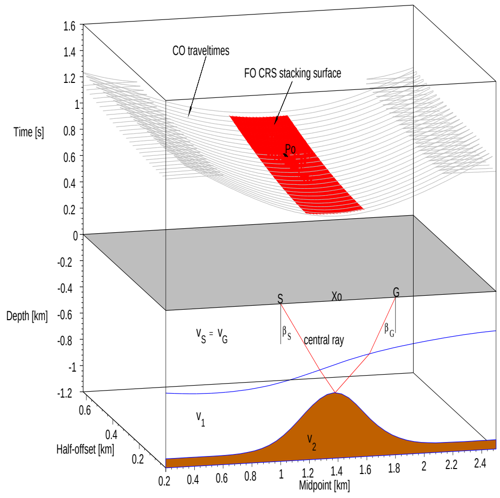

Figure 1: Upper part: Example of P-P kinematic reflection response from the dome-like reflector represented by the CO traveltime curves (grey). The reflection response is approximated by the FO CRS stacking surface. Lower part: a 2D medium consisting of two homogeneous layers about a half-space, bounded by curved interfaces.

Sensibility Analysis

The most important step to obtain a simulated finite-offset section by the FO CRS stack traveltime is to perform an accurate and efficient parameter search of these five parameters. We investigate how sensitive is the operator on the variations of the searched-for parameters. This is done by analysing the first derivative of the moveout formula (1) with respect to each one of the parameters.

These derivatives, are shown in the Figures 3 to 8. We remind that in this analysis we considered for a fixed point $P_0(x_0 = 1.4km, h_0 = 0.4km, t_0 = 0.7364s.)$ (Figure 1). The traveltime derivative with respect to β_S presents higher positive values at smaller and larger offsets and midpoints far from central point P_0. This does not occur with the derivate with respect to β_G, which presents smaller negative and positive values. The traveltime derivative with respect to K_1 presents higher positive values at smaller and larger offsets and midpoint far from central point. The same does not occur with the derivative with respect to K_2, where the values are negatives. Finally, the derivative with respect to K_3 presents negative values at smaller and larger offsets and midpoint near and far from the central point. This last derivate also presents smaller positive values at larger offsets.

Conclusions

By using traveltime derivatives of the FO CRS traveltime approximation, we have analyzed the sensibility of the operator with respect to each of the searched-for parameter.

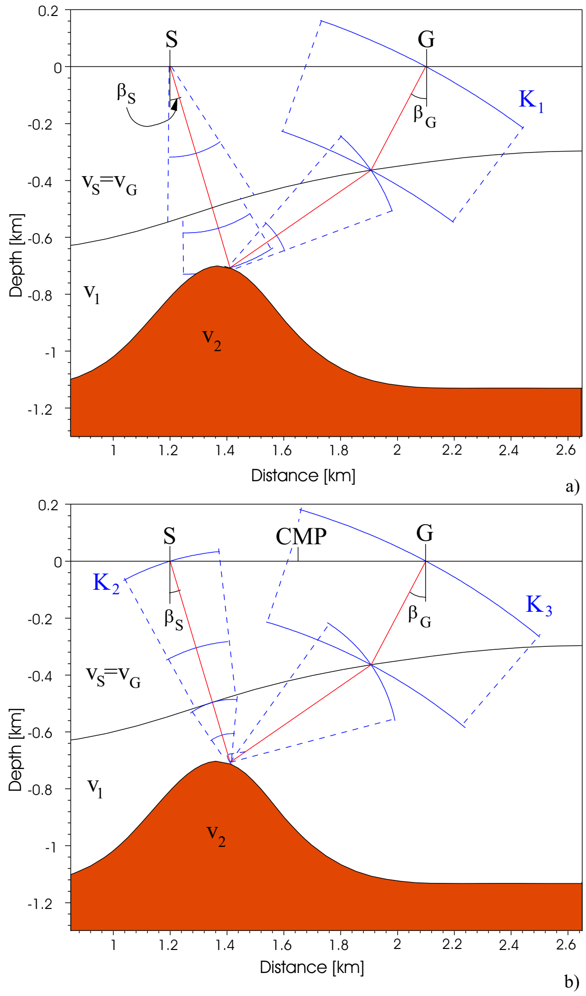

Figure 2: Wavefront curvatures (K_1, K_2 and K_3) associated to two experiments: a) real CS experiment, and b)hypothetical CMP experiment in an isotropic model with constant-velocity layers (modified from Bergler et al. (2001b)).

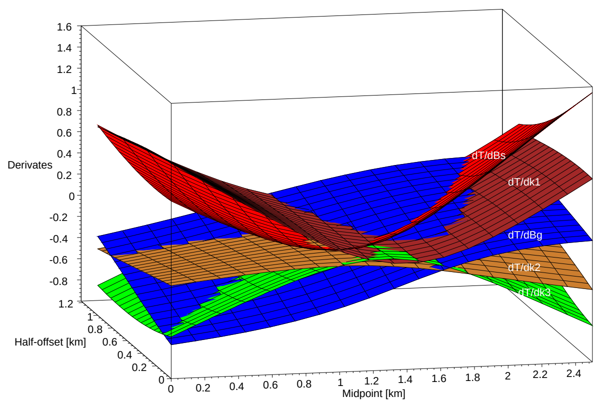

Figure 3: FO CRS traveltime derivates for the five stacking parameters.

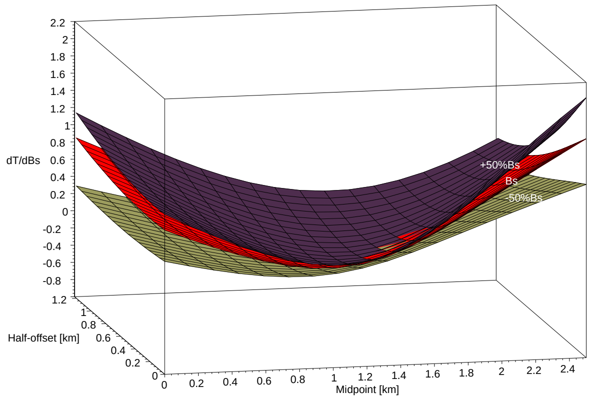

Figure 4: FO CRS traveltime derivates by using variations (-50, $+50$ percentages) and true values in the angle β_S, between half-offset: 0-1.2 km in increments of 0.025 km.

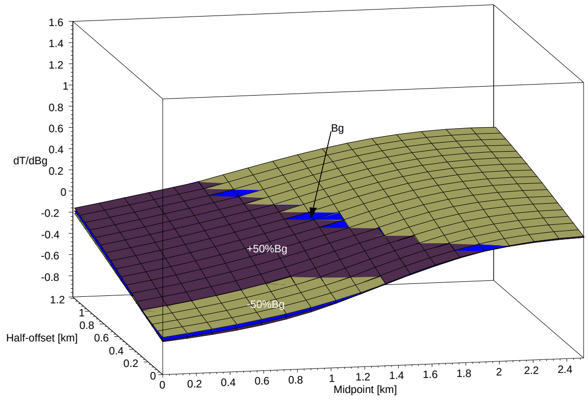

Figure 5: FO CRS traveltime derivates by using variations (-50, $+50$ percentages) and true values in the angle β_G, between half-offset: 0-1.2 km in increments of 0.025 km.

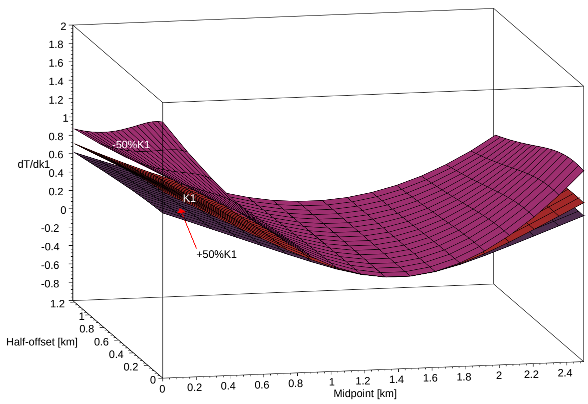

Figure 6: The FO CRS stacking surface by using variations (-50, $+50$ percentages) and true values in the wavefront curvature K_1, between half-offset: 0-1.2 km in increments of 0.025 km.

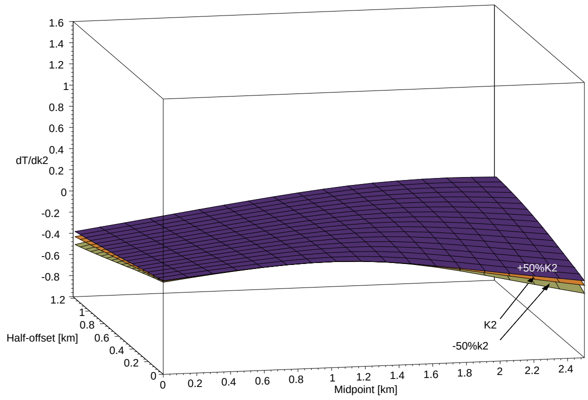

Figure 7: The FO CRS stacking surface by using variations (-50, $+50$ percentages) and true values in the wavefront curvatures K_2, between half-offset: 0-1.2 km in increments of 0.025 km.

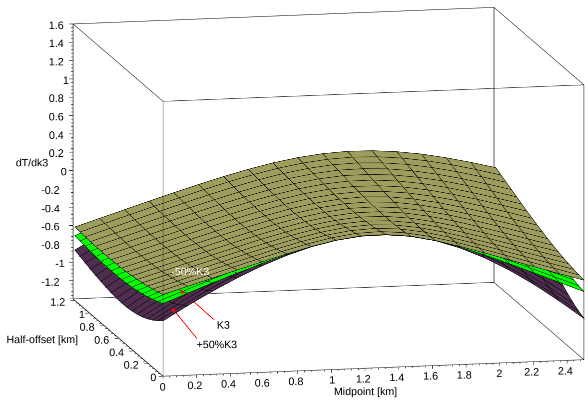

Figure 8: The FO CRS stacking surface by using variations (-50, $+50$ percentages) and true values in the wavefront curvatures K_3, between half-offset: 0-1.2 km in increments of 0.025 km.

For the central point studied the traveltime function is very sensitive to the β_S and K_1. This is an indicator that both parameters (β_S, K_1) can be very well determined by the inverse problem solution. In the case of the parameters β_G, K_2 and K_3, this operator is less sensitive. In this case these parameters are poorly determined during the search procedure, that suggests to use some constraint to better determining the parameters β_G, K_2 and K_3.

Acknowledgments

We thank the support of the WIT Consortium (Germany).

References

Bergler, S., Duveneck, E., Höcht, G., Zhang, Y., and Hubral, P., 2001a, Common-reflection-surface stack for converted waves: Wave Inversion Technology (WIT) Report (Germany), pages 24–31.

——— 2001b, Common-reflection-surface stack for common-offset: practical aspects: 63rd Annual Internat. Mtg., Soc. Expl. Geophys., Expanded Abstracts, P 076.

de Bazelaire, E., 1988, Normal moveout revisited – inhomogeneous media and curved interfaces: Geophysics, **53**, no. 2, 143–157.

Gelchinsky, B., Berkovitch, A., and Keydar, S., 1999a, Multifocusing homeomorphic imaging. Part I. Basic concepts and formulas. Special Issue: Macro-Model Independent Seismic Reflection Imaging: J. Appl. Geoph., **42**, no. 3,4, 229–242.

——— 1999b, Multifocusing homeomorphic imaging. Part II. Multifold data set and Multifocusing. Special Issue: Macro-Model Independent Seismic Reflection Imaging: J. Appl. Geoph., **42**, no. 3,4, 243–260.

Jäger, R., Mann, J., Höcht, G., and Hubral, P., 2001, Common-reflection-surface stack: Image and attributes: Geophysics, **66**, no. 1, 97–109.

Landa, E., Gurevich, B., Keydar, S., and Trachman, P., 1999, Multifocusing Stack - a New Time Imaging Method: 6th Annual Congress, SBGf, Expanded Abstracts, 195.

Mann, J., Jäger, R., Müller, T., Höcht, G., and Hubral, P., 1999, Common-reflection-surface stack - a real data example: J. Appl. Geoph., **42**, no. 3,4, 301–318.

Trappe, H., Gierse, G., and Pruessmann, J., 2001, Case studies show potential of common reflection surface stack - structural resolution in the time domain beyond the conventional nmo/dmo stack.: First Break, **27**, no. 19, 625–633.

Zhang, Y., Bergler, S., and Hubral, P., 2001, Common-reflection-surface (crs) stack for common-offset: Geophysical Prospecting, **49**, 709–718.